

EFFECTS OF CHEMICAL REACTION ON TRANSIENT MHD FLOW WITH MASS TRANSFER PAST AN IMPULSIVELY FIXED INFINITE VERTICAL PLATE IN THE PRESENCE OF THERMAL RADIATION

B. PRABHAKAR REDDY

Department of Mathematics
College of Natural and Mathematical Sciences
The University of Dodoma
P. Box. No. 338, Dodoma, TANZANIA

Department of Mathematics
Geethanjali College of Engineering and Technology
Cheeryal (V), Keesara (M), Medchal (Dist) -501301
Telangana, INDIA
E-mail: prabhakar.bijjula@gmail.com

The effects of chemical reaction on a transient MHD mixed convection flow with mass transfer past an impulsively fixed infinite vertical plate under the influence of a transverse magnetic field have been presented. The medium is considered to be non-scattering and the fluid to be non-gray having emitting-absorbing and optically thick radiation limit properties. The dimensionless governing equations of the flow and mass transfer with boundary conditions are solved numerically by using the Ritz finite element method. The numerical results for the velocity, temperature and the concentration profiles as well as the skin-friction coefficient for different values of physical parameters such as the radiation parameter, magnetic parameter, Schmidt number and chemical reaction parameter have been obtained and presented through graphs and tables. It has been found that there is a fall in the temperature and velocity for both air and water as the radiation parameter is increased. An increase in the Schmidt number and chemical reaction parameter results a decrease in the concentration and velocity profiles for both air and water. Furthermore, an increase in the radiation parameter, magnetic parameter, Schmidt number and chemical reaction parameter decreases the skin-friction.

Key words: MHD, magnetic field, fixed vertical plate, chemical reaction parameter, radiation parameter.

1. Introduction

In recent years, considerable interest is has been shown in the study of heat and mass transfer in the presence of chemical reaction. There are many transport processes that are governed by the combined action of buoyancy forces due to both thermal and mass diffusion in the presence of chemical reaction effect. These processes are observed in nuclear reactor safety and combustion systems, solar collectors, as well as metallurgical and chemical engineering. Their other applications include solidification of binary alloys and crystal growth dispersion of dissolved materials, drying and dehydration operations in chemical and food processing plants, and combustion of atomized liquid fuels.

The effects of chemical reaction on heat and mass transfer in a laminar boundary layer flow have been studied under different conditions by several authors [1-4]. Muthucumaraswamy and Meenakshisundaram [5] investigated the chemical reaction effects on a vertical oscillating plate with variable temperature by the Laplace transform technique. The chemical reaction, heat and mass transfer on an MHD flow over a vertical isothermal cone surface in a micro-polar fluid with heat generation/absorption were reported by Kabier and Abdou [6]. The effects of chemical reaction on a transient MHD free convection over

a moving vertical plate were presented by Al-Odat and Al-Azab [7]. Mahapatra *et al.* [8] analyzed the effects of chemical reaction on a free convection flow through a porous medium bounded by a vertical surface. Similarity solutions for the unsteady MHD flow near a stagnation point of a three dimensional porous body with heat and mass transfer, heat generation/absorption and chemical reaction were provided by Chamkha and Ahmed [9]. Devika *et al.* [10] studied an MHD oscillatory flow of a visco-elastic fluid in a porous channel with chemical reaction.

The radiative heat and mass transfer play an important role in manufacturing industries for the design of gas turbines, missiles, satellites, nuclear power plants and various propulsion devices for aircrafts, material processing, energy utilization, food processing and cryogenic engineering as well as numerous agricultural, health and military applications. The problem of laminar convective flow in a vertical heated channel in optically thin limit was studied by Grief *et al.* [11]. Ali *et al.* [12] investigated the radiation effects on a natural convection flow over a vertical surface in a gray gas. The problem of interaction of mixed convection with thermal radiation in a laminar boundary layer flow over a horizontal, continuously moving sheet with suction/injection was reported by Mansor [13]. Abd-El-Naby *et al.* [14] analyzed the effects of radiation on an MHD free convection flow over a vertical plate with variable surface temperature by the finite difference method. Chandrakala and Raj [15] investigated the radiation effects on an MHD flow past an impulsively started infinite isothermal vertical plate. Thermal radiation effects on a transient MHD flow with mass transfer past an impulsively fixed infinite vertical plate were presented by Ahmed and Sarmah [16]. The effects of thermal radiation on an unsteady mixed convection flow and heat transfer over a porous stretching surface in a porous medium was presented by Mukhopadhyay [17]. Rao and Reddy [18] presented the finite element analysis of heat and mass transfer of an unsteady MHD natural convection flow of a rotating fluid past a vertical porous plate in the presence of radiative heat transfer. Seth *et al.* [19] studied the unsteady MHD free convection flow with radiative heat transfer past an impulsively moving plate with ramped wall temperature. Recently, Muthucumaraswamy and Sivakumar [20] studied an MHD flow past a parabolic flow past an infinite isothermal vertical plate in the presence of thermal radiation and chemical reaction.

The aim of the present work is to analyze the effects of chemical reaction on an unsteady transient MHD mixed convection flow with mass transfer past an impulsively fixed infinite vertical plate in the presence of thermal radiation. The Ritz finite element method has been adopted to solve the governing boundary layer equations of the flow under the boundary conditions, which is more economical from computational point of view. The effects of the physical parameters on the velocity, temperature and the concentration profiles have been presented through the graphs. The numerical data for the skin-friction coefficient in the direction of the flow have been tabulated and then discussed.

2. Basic equations of the flow

Consider the unsteady mixed convection flow with mass transfer of a viscous, incompressible, electrically conducting fluid flow past a suddenly held fixed infinite vertical plate in the presence of thermal radiation. The flow is assumed to be in the x' -direction, which is taken along the plate in the upward vertical direction and the y' -axis is taken to be normal to the plate directed into the fluid region. The plate is also subjected to a uniform magnetic field of strength B_0 which is assumed to be applied normal to the plate. The magnetic Reynolds number is assumed to be so small that the induced magnetic field can be neglected. Initially ($t' \leq 0$), the plate and surrounding gas were at the same temperature T_∞' with the concentration level C_∞' at all points and the plate was moving parallel to itself with velocity U_0' . Subsequently, at time $t' > 0$, the plate is suddenly made stationary and the plate temperature rises to T_w' and the concentration level at the plate rises to C_w' . Under the usual boundary layer and Boussinesq approximations, the governing equations of the radiating and chemically reacting fluid are

$$\frac{\partial w'}{\partial t'} = -g\beta(T' - T'_\infty) - g\beta^*(C' - C'_\infty) + \nu \frac{\partial^2 w'}{\partial y'^2} - \frac{\sigma B_0^2 w'}{\rho}, \quad (2.1)$$

$$\frac{\partial T'}{\partial t'} = \frac{k}{\rho C_p} \frac{\partial^2 T'}{\partial y'^2} - \frac{l}{\rho C_p} \frac{\partial q_r}{\partial y'}, \quad (2.2)$$

$$\frac{\partial C'}{\partial t'} = D \frac{\partial^2 C'}{\partial y'^2} - \delta'(C' - C'_\infty) \quad (2.3)$$

where $w' = U'_o - u'$ (2.4)

with the initial and boundary conditions

$$\begin{aligned} t' \leq 0; \quad w' = 0, \quad T' = T'_\infty, \quad C' = C'_\infty \quad \text{for all } y', \\ t' > 0; \quad w' = U'_o, \quad T' = T'_w, \quad C' = C'_w \quad \text{at } y' = 0, \\ w' = 0, \quad T' = T'_\infty, \quad C' = C'_\infty \quad \text{as } y' \rightarrow \infty. \end{aligned} \quad (2.5)$$

In case of optically thick limit, the fluid cannot absorb its own emitted radiation, but it absorbs the radiation emitted by the boundaries. The radiation flux in the optically thick limit for a non-gray gas near equilibrium is given by

$$\frac{\partial q_r}{\partial y'} = 4I(T' - T'_\infty) \quad (2.6)$$

where

$$I = \int_0^\infty K_{\lambda w} \left(\frac{de_{b\lambda}}{dT'} \right) d\lambda \quad (2.7)$$

where $K_{\lambda w}$ is the absorption coefficient and $e_{\lambda b}$ is the Plank function.

We now introduce the following non-dimensional quantities.

$$\begin{aligned} w = \frac{w'}{U'_o}, \quad y = \frac{y' U'_o}{\nu}, \quad t = \frac{t' U'^2_0}{\nu}, \quad u = \frac{u'}{U'_o}, \quad \text{Sc} = \frac{\nu}{D}, \quad \text{Pr} = \frac{\mu C_p}{k}, \\ \lambda = \frac{4I\nu^2}{kU'^2_0}, \quad M = \frac{\sigma B_0^2 \nu}{\rho U'^2_0}, \quad \theta = \frac{(T' - T'_\infty)}{(T'_w - T'_\infty)}, \quad \phi = \frac{(C' - C'_\infty)}{(C'_w - C'_\infty)}, \\ \delta = \frac{\delta' \nu}{U'^2_0}, \quad \text{Gr} = \frac{g\beta\nu(T'_w - T'_\infty)}{U'^2_0}, \quad \text{Gm} = \frac{g\beta\nu(C'_w - C'_\infty)}{U'^2_0}. \end{aligned} \quad (2.8)$$

Using Eqs (2.6), (2.7) and (2.8) in Eqs (2.1)-(2.5), we obtain the following non-dimensional governing equations of the flow

$$\frac{\partial w}{\partial t} = -Gr\theta - Gm\phi + \frac{\partial^2 w}{\partial y^2} - Mw, \quad (2.9)$$

$$Pr \frac{\partial \theta}{\partial t} = \frac{\partial^2 \theta}{\partial y^2} - \lambda\theta, \quad (2.10)$$

$$\frac{\partial \phi}{\partial t} = \frac{I}{Sc} \frac{\partial^2 \phi}{\partial y^2} - \delta\phi \quad (2.11)$$

where $w = 1 - u$. (2.12)

The corresponding boundary conditions in non-dimensional form are

$$\begin{aligned} t \leq 0; \quad w = 0, \quad \theta = 0, \quad \phi = 0 \quad \text{for all } y, \\ t > 0; \quad w = 1, \quad \theta = 1, \quad \phi = 1 \quad \text{at } y = 0, \\ w = 0, \quad \theta = 0, \quad \phi = 0 \quad \text{as } y \rightarrow \infty. \end{aligned} \quad (2.13)$$

3. Method of solution

Using Eq.(2.12) in the Eq.(2.9) and then applying the Ritz finite element method to the resulting equation over the two-nodded linear element (e) , $(y_j \leq y \leq y_k)$, we have

$$J^{(e)}(u) = \frac{I}{2} \int_{y_j}^{y_k} \left\{ \left(\frac{\partial u^{(e)}}{\partial y} \right)^2 + Mu^{(e)2} + 2u^{(e)} \frac{\partial u^{(e)}}{\partial t} - 2u^{(e)} \Delta \right\} dy = \text{minimum} \quad (3.1)$$

where $\Delta = (Gr\theta + Gm\phi - M)$.

Let $u^{(e)} = \psi_j(y)u_j(t) + \psi_k(y)u_k(t) = \psi_j u_j + \psi_k u_k$ be the linear approximation solution over the element (e) , $(y_j \leq y \leq y_k)$. From Eq.(3.1) the element equation is given by

$$\begin{aligned} \int_{y_j}^{y_k} \begin{bmatrix} \psi_j' \psi_j' & \psi_j' \psi_k' \\ \psi_k' \psi_j' & \psi_k' \psi_k' \end{bmatrix} \begin{bmatrix} u_j \\ u_k \end{bmatrix} dy + M \int_{y_j}^{y_k} \begin{bmatrix} \psi_j \psi_j & \psi_j \psi_k \\ \psi_k \psi_j & \psi_k \psi_k \end{bmatrix} \begin{bmatrix} u_j \\ u_k \end{bmatrix} dy + \\ + \int_{y_j}^{y_k} \begin{bmatrix} \psi_j \psi_j & \psi_j \psi_k \\ \psi_k \psi_j & \psi_k \psi_k \end{bmatrix} \begin{bmatrix} \dot{u}_j \\ \dot{u}_k \end{bmatrix} dy - \Delta \int_{y_j}^{y_k} \begin{bmatrix} \psi_j \\ \psi_k \end{bmatrix} dy = 0 \end{aligned}$$

where the prime and the dot denotes the differentiation with respect to y and t , respectively. Simplifying yields

$$\frac{1}{l^{(e)}} \begin{bmatrix} 1 & -1 \\ -1 & 1 \end{bmatrix} \begin{bmatrix} u_j \\ u_k \end{bmatrix} + \frac{Ml^{(e)}}{6} \begin{bmatrix} 2 & 1 \\ 1 & 2 \end{bmatrix} \begin{bmatrix} u_j \\ u_k \end{bmatrix} + \frac{l^{(e)}}{6} \begin{bmatrix} 2 & 1 \\ 1 & 2 \end{bmatrix} \begin{bmatrix} u_j^\bullet \\ u_k^\bullet \end{bmatrix} - \Delta \frac{l^{(e)}}{2} \begin{bmatrix} 1 \\ 1 \end{bmatrix} = 0$$

where $l^{(e)} = y_k - y_j$ is the length of the element (e). In order to get the difference equation at the node i , we write the element equations for two consecutive elements $y_{i-1} \leq y \leq y_i$ and $y_i \leq y \leq y_{i+1}$, assembling these two resulting element equations, we obtain

$$\frac{1}{l^{(e)}} \begin{bmatrix} 1 & -1 & 0 \\ -1 & 2 & -1 \\ 0 & -1 & 1 \end{bmatrix} \begin{bmatrix} u_{i-1} \\ u_i \\ u_{i+1} \end{bmatrix} + \frac{Ml^{(e)}}{6} \begin{bmatrix} 2 & 1 & 0 \\ 1 & 4 & 1 \\ 0 & 1 & 2 \end{bmatrix} \begin{bmatrix} u_{i-1} \\ u_i \\ u_{i+1} \end{bmatrix} + \frac{l^{(e)}}{6} \begin{bmatrix} 2 & 1 & 0 \\ 1 & 4 & 1 \\ 0 & 1 & 2 \end{bmatrix} \begin{bmatrix} u_{i-1}^\bullet \\ u_i^\bullet \\ u_{i+1}^\bullet \end{bmatrix} = \Delta \frac{l^{(e)}}{2} \begin{bmatrix} 1 \\ 2 \\ 1 \end{bmatrix}. \quad (3.2)$$

Putting the row corresponding to the node i to zero in Eq.(3.2) the following difference schemes with $l^{(e)} = h$ are obtained

$$(u_{i-1}^\bullet + 4u_i^\bullet + u_{i+1}^\bullet) = \frac{1}{h^2}(6 - Mh^2)(u_{i-1} + u_{i+1}) + \frac{1}{h^2}(12 + 4Mh^2)u_i + 6\Delta. \quad (3.3)$$

Applying the trapezoidal rule to Eq.(3.3) the following system of equations is obtained in the Crank-Nicholson method

$$\left(1 - 3r + \frac{1}{2}rMh^2\right)u_{i-1}^{j+1} + (4 + 6r + 2rMh^2)u_i^{j+1} + \left(1 - 3r + \frac{1}{2}rMh^2\right)u_{i+1}^{j+1} = \Omega_{1i}^j. \quad (3.4)$$

Applying the similar procedure to Eq.(2.10) and (2.11) we obtain

$$\left(\text{Pr} - 3r + \frac{1}{2}r\lambda h^2\right)\theta_{i-1}^{j+1} + (4\text{Pr} + 6r + 2r\lambda h^2)\theta_i^{j+1} + \left(\text{Pr} - 3r + \frac{1}{2}r\lambda h^2\right)\theta_{i+1}^{j+1} = \Omega_{2i}^j, \quad (3.5)$$

$$\begin{aligned} &\left(\text{Sc} - 3r + \frac{1}{2}r\text{Sc}\delta h^2\right)\phi_{i-1}^{j+1} + (4\text{Sc} + 6r + 2r\text{Sc}\delta h^2)\phi_i^{j+1} + \\ &+ \left(\text{Sc} - 3r + \frac{1}{2}r\text{Sc}\delta h^2\right)\phi_{i+1}^{j+1} = \Omega_{3i}^j \end{aligned} \quad (3.6)$$

where

$$\begin{aligned} \Omega_{1i}^j = &\left(1 + 3r - \frac{1}{2}rMh^2\right)u_{i-1}^j + (4 - 6r - 2rMh^2)u_i^j + \\ &+ \left(1 + 3r - \frac{1}{2}rMh^2\right)u_{i+1}^j + 6k(\text{Gr}\theta_i^j + \text{Gm}\phi_i^j - M), \end{aligned}$$

$$\Omega_{2i}^j = \left(\text{Pr} + 3r - \frac{1}{2} r \lambda h^2 \right) \theta_{i-1}^j + \left(4\text{Pr} - 6r - 2r \lambda h^2 \right) \theta_i^j + \left(\text{Pr} + 3r - \frac{1}{2} r \lambda h^2 \right) \theta_{i+1}^j,$$

$$\Omega_{3i}^j = \left(\text{Sc} + 3r - \frac{1}{2} r \text{Sc} \delta h^2 \right) \phi_{i-1}^j + \left(4\text{Sc} - 6r - 2r \text{Sc} \delta h^2 \right) \phi_i^j + \left(\text{Sc} + 3r - \frac{1}{2} r \text{Sc} \delta h^2 \right) \phi_{i+1}^j.$$

Here, $r = \frac{k}{h^2}$ and h, k are mesh sizes along the y - direction and time t - direction, respectively. The index i refers to the space and j refers to the time. In Eqs (3.4)-(3.6) taking $i = I(I)n$ and using boundary conditions (2.13), the following tri-diagonal systems of equations are obtained

$$\begin{aligned} Au &= A' \\ B\theta &= B' \\ C\phi &= C' \end{aligned} \tag{3.7}$$

where A, B and C are tri-diagonal matrices of order - n and whose elements are given by

$$\begin{aligned} a_{i,i} &= 4 + 6r + 2rMh^2; \\ b_{i,i} &= 4\text{Pr} + 6r + 2r\lambda h^2; \quad \text{at} \quad i = I(I)n; \\ c_{i,i} &= 4\text{Sc} + 6r + 2r\text{Sc} \delta h^2; \\ a_{i-1,j} &= a_{i,j-1} = 1 - 3r + \frac{1}{2} rMh^2; \\ b_{i-1,j} &= b_{i,j-1} = \text{Pr} - 3r + \frac{1}{2} r\lambda h^2; \quad \text{at} \quad i = 2(I)n; \\ c_{i-1,j} &= c_{i,j-1} = \text{Sc} - 3r + \frac{1}{2} r\text{Sc} \delta h^2. \end{aligned}$$

Here u, θ, ϕ and A', B', C' are column matrices having the n - components $u_i^{j+1}, \theta_i^{j+1}, \phi_i^{j+1}$ and $u_i^j, \theta_i^j, \phi_i^j$, respectively. The above tri-diagonal systems of Eqs (3.7) are solved by using the Thomas algorithm. The numerical solutions for the velocity, temperature and the concentration profiles are obtained by using C - program. The boundary condition $y \rightarrow \infty$ is approximated by $y_{\max} = 10$, which is sufficiently large for the velocity to approach the convergence criterion. To judge the convergence and stability of the Ritz finite element method, computations are carried out by making small changes in the values of h and k by running the same program, no significant change was observed in the values of u, θ and ϕ . Hence, we conclude that the Ritz finite element method is convergent and stable.

The non-dimensional skin-friction at the plate is given by $\tau = - \left(\frac{\partial u}{\partial y} \right)_{y=0}$.

4. Results and discussion

To gain a perspective of the physics of the flow regime, we have computed the numerical results for the velocity, temperature and concentration profiles as well as the skin-friction coefficient for different values of the material parameters involved in the problem under the investigation. The obtained numerical results have been presented through graphs and tables. The fluids considered in this study are air and water ($Pr = 0.71$ and 7.0 , respectively at $20^{\circ}C$). The value of the Schmidt number (Sc) is taken as 0.60 which corresponds to water-vapour and represents a diffusing chemical species of most common interest in air. Throughout the investigation the values of the Grashof number for heat transfer (Gr) and the Grashof number for mass transfer (Gm) are considered to be 10.0 and 5.0 (externally cooled plate) and the time t is fixed at $t = 1.0$. The values of the other parameters viz, the magnetic parameter (M), radiation parameter (λ) and chemical reaction parameter (δ) are selected arbitrarily.

The effects of the radiation parameter (λ) on the velocity profiles for air and water are illustrated in Figs 1 and 2, respectively. It is seen from these figures that with an increase in the radiation parameter from 1 to 3 and then to 5, the fluid velocity decreases for both air and water. Also, we observe that in case of air, the fluid velocity increases quickly up to some thin layer of the fluid adjacent to the plate and after this fluid layer the velocity of the fluid asymptotically decreases to 1 as $y \rightarrow \infty$. Figures 3 and 4 show the effect of the magnetic parameter (M) on the velocity profiles for air and water, respectively. It is observed from these figures that the velocity of the fluid decreases for increasing values of the magnetic parameter. It is interesting that in case of water the strength of the applied magnetic field is small or moderate; the velocity of the fluid decreases with the increasing magnetic parameter near the plate after that it begins to flow in the upward direction. The effects of the Schmidt number $Sc = 0.22, 0.60$ and 0.78 , which correspond to hydrogen, water-vapour and ammonia, respectively on the velocity profiles for air and water are shown in Figs 5 and 6, respectively. It can be seen from these figures that an increase in the Schmidt number leads to a decrease in the velocity of the fluid for both air and water. The velocity of the fluid is higher for hydrogen than water-vapour and ammonia. Figures 7 and 8 display the effects of the chemical reaction parameter (δ) on the velocity profiles for air and water, respectively. It is clear that the fluid velocity decreases as the chemical reaction parameter δ increases for both air and water. From all the figures, we notice that the velocity is higher for air than water for different parameters. Also, the effects of λ, M, Sc and δ on the velocity profiles for large y are negligible irrespective of the fluid being air or water.

Figures 9 and 10 represent the effects of the radiation parameter (λ) on the temperature distribution θ against y for air and water, respectively. It is noticed from these figures that with an increase in the radiation parameter there is a fall in the temperature for both air and water. Also, we observe that the temperature decreases asymptotically from 1 to 0 as y increases. The effect of λ on the temperature is more pronounced in the case of air than water.

The variation of the concentration profiles ϕ with the Schmidt number (Sc) against y is presented in Fig.11. It is evident from this figure that as the Schmidt number is increased the concentration and concentration boundary layer are both seen to a decrease. Physically, an increase in the Schmidt number leads to decrease in the molecular diffusivity and results in a decrease of the concentration boundary layer. The effects of the chemical reaction parameter (δ) on the concentration profiles are shown in Fig.12. It is observed that a decrease from a maximum at the wall ($1, 0$) to a minimum value happens with maximum distance y . However, with increasing the chemical reaction parameter, we observe that there is a decrease in the concentration profiles.

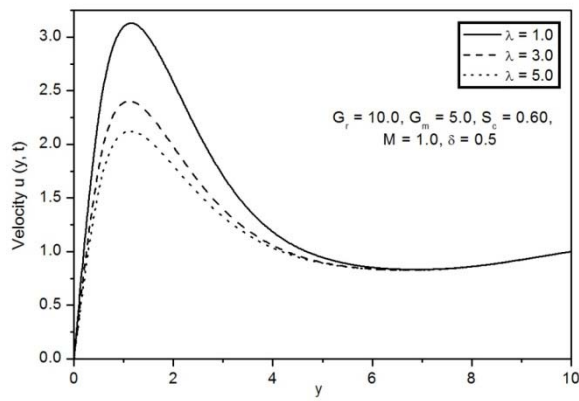


Fig.1. Effects of the radiation parameter (λ) on the velocity profiles against y for air ($Pr = 0.71$).

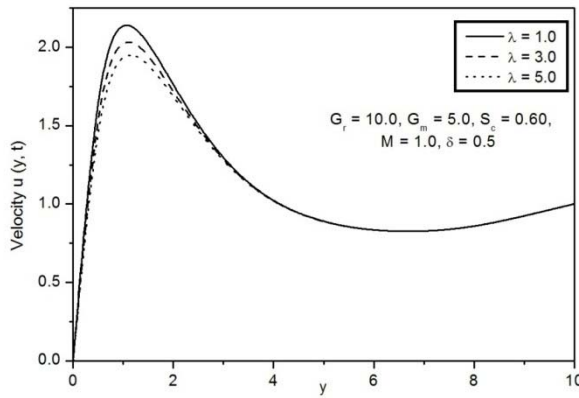


Fig.2. Effects of the radiation parameter (λ) on the velocity profiles against y for water ($Pr = 7.0$).

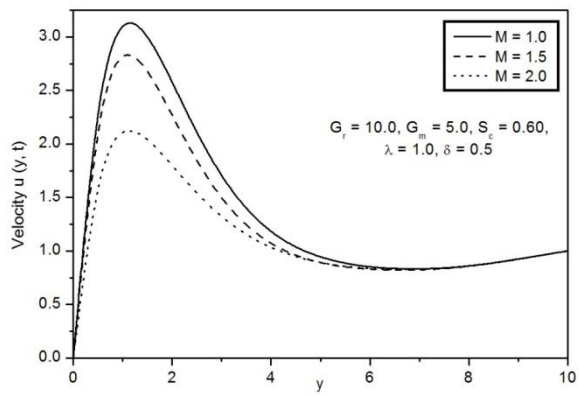


Fig.3. Effects of the magnetic parameter (M) on the velocity profiles against y for air ($Pr = 0.71$).

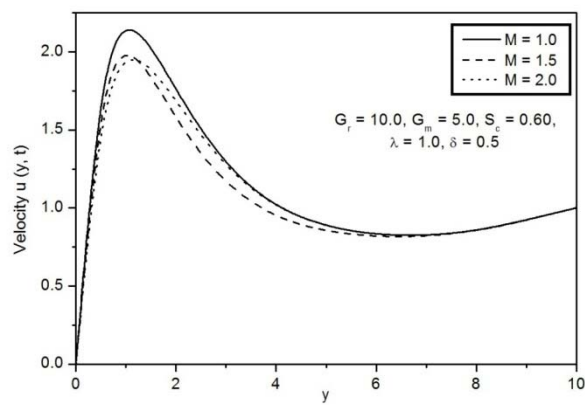


Fig.4. Effects of the magnetic parameter (M) on the velocity profiles against y for water ($Pr = 7.0$).

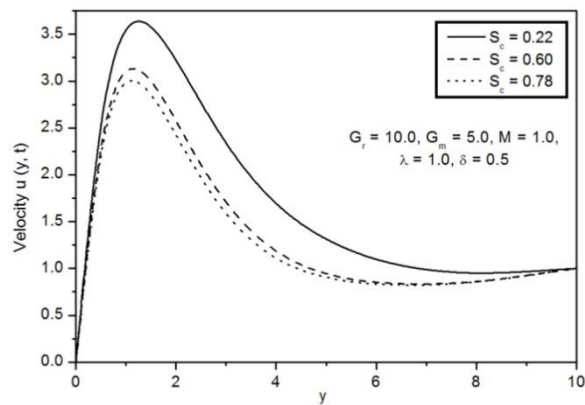


Fig.5. Effects of the Schmidt number (Sc) on the velocity profiles against y for air ($Pr = 0.71$).

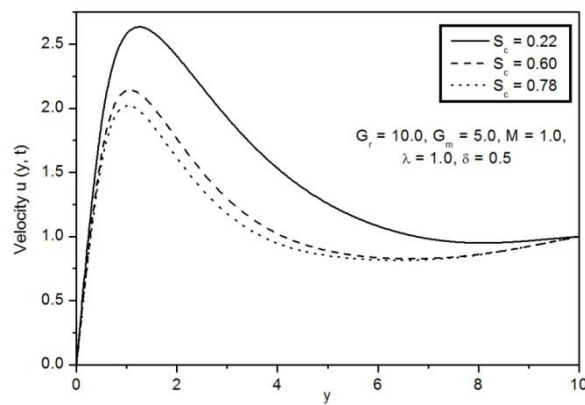


Fig.6. Effects of the Schmidt number (Sc) on the velocity profiles against y for water ($Pr = 7.0$).

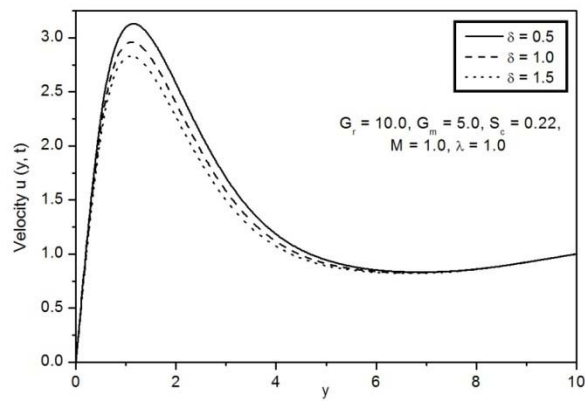


Fig.7. Effects of the chemical reaction parameter (δ) on the velocity profiles against y for air ($Pr = 0.71$).

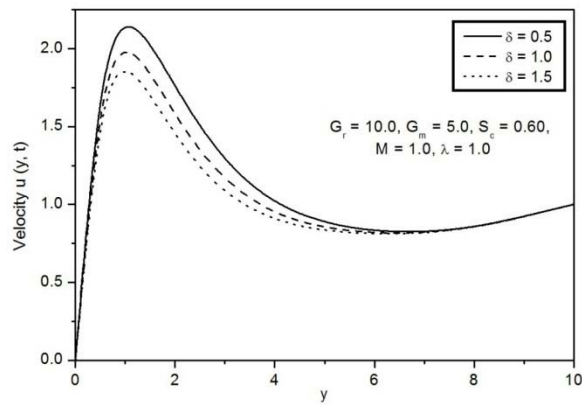


Fig.8. Effects of the chemical reaction parameter (δ) on the velocity profiles against y for water ($Pr = 7.0$).

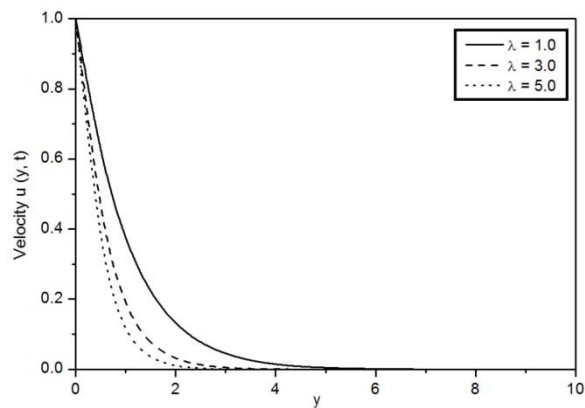


Fig.9. Effects of the radiation parameter (λ) on the temperature profiles against y for air ($Pr = 0.71$).

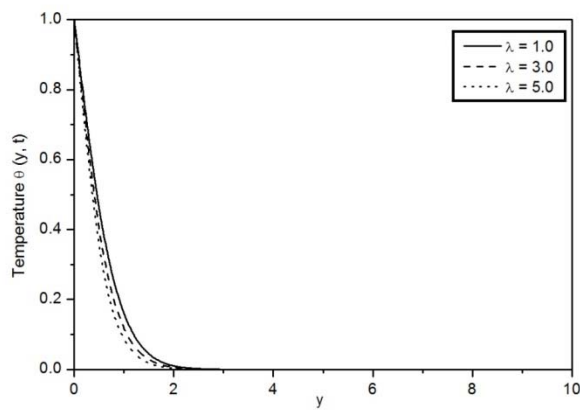


Fig.10. Effects of the radiation parameter (λ) on the temperature profiles against y for water ($Pr = 7.0$).

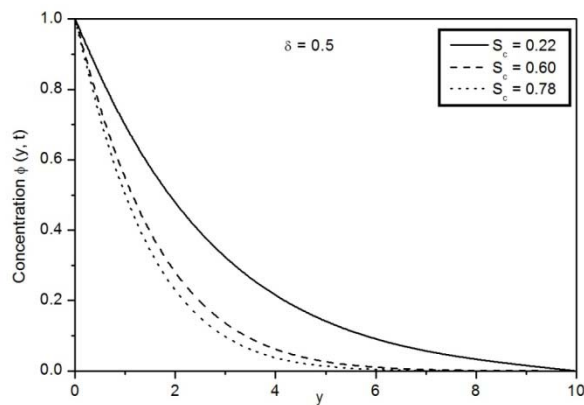


Fig.11. Effects of the Schmidt number (Sc) on the concentration profiles against y when $\delta = 0.5$.

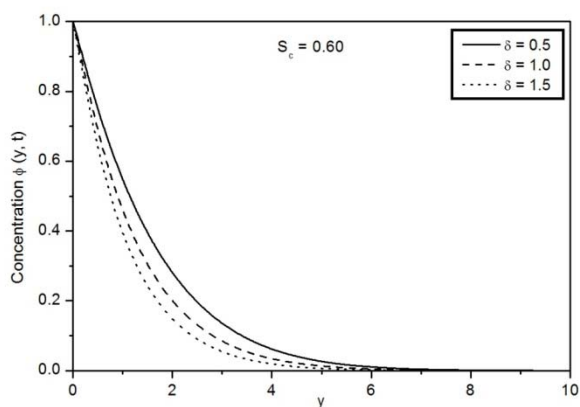


Fig.12. Effects of the chemical reaction parameter (δ) on the concentration profiles against y when $Sc = 0.60$.

The effects of λ and M on the skin-friction coefficient (τ) for air and water are presented in Tab.1. It is clear from this table that increasing values of the radiation parameter or magnetic parameter decrease the

skin-friction coefficient irrespective of the fluid being air or water. Table 2 shows the effects of Sc and δ on the skin-friction for air and water. It is observed from this table that an increase in the Schmidt number or chemical reaction parameter decreases the skin-friction coefficient for both air and water. Also, the skin-friction is more for air than water.

Table 1. Effects of λ and M on the skin-friction coefficient (τ) for air and water when $Gr = 10.0$, $Gm = 5.0$, $Sc = 0.60$ and $\delta = 0.5$.

Pr	λ/M	1.0	3.0	5.0
0.71	1.0	5.198340	4.134522	3.639960
	1.5	4.127504	3.337836	2.964300
	2.0	3.256002	2.673114	2.390402
7.00	1.0	3.814770	3.561600	3.356276
	1.5	3.153782	2.943166	2.772602
	2.0	2.569116	2.396744	2.257178

Table 2. Effects of Sc and δ on the skin-friction coefficient (τ) for air and water when $Gr = 10.0$, $Gm = 5.0$, $\lambda = 1.0$ and $M = 1.0$.

Pr	Sc/δ	0.22	0.60	0.78
0.71	0.5	5.705632	5.198340	5.055094
	1.0	5.522080	4.990514	4.845006
	1.5	5.372182	4.826464	4.680690
7.00	0.5	4.322062	3.814770	3.671524
	1.0	4.138510	3.606944	3.461438
	1.5	3.988612	3.442894	3.297120

4. Conclusion

In this study, the unsteady transient hydro-magnetic mixed convection with mass transfer flow of a radiating and chemically reacting fluid past an impulsively fixed infinite vertical plate under the influence of a transverse magnetic field is discussed. Employing the Ritz finite element method the leading equations have been solved numerically. We have computed the numerical results for the velocity, temperature and concentration profiles as well as the skin-friction coefficient for different physical parameters and the computed results are presented through graphs and tables. We can conclude from these results that the radiation indeed affects the temperature and therefore velocity for both air and water, hence the skin-friction. An increase in the Schmidt number results in a decrease of the velocity for both air and water and also species concentration. Increasing values of the magnetic parameter decrease the fluid velocity for air and in the case of water it decreases near the plate after that the fluid starts to flow in the upward direction. An increase in the chemical reaction parameter decreases the fluid velocity and concentration for both air and water. The skin-friction coefficient decreases with an increase in the radiation parameter or magnetic parameter or Schmidt number or chemical reaction parameter for both air and water.

Nomenclature

C'	– species concentration in the fluid kgm^{-3}
C_p	– specific heat at constant pressure $J kg^{-1}k$
C_w'	– species concentration at the plate
C_∞'	– concentration in the fluid far away from the plate
D	– mass diffusion m^2s^{-1}
Gm	– Grashof number for mass transfer
Gr	– Grashof number for heat transfer
g	– acceleration due to gravity ms^{-2}
k	– thermal conductivity $Wm^{-1}s^{-1}$
M	– magnetic parameter
Pr	– Prandtl number
q_r	– radiative flux
Sc	– Schmidt number
T'	– temperature of the fluid K
T_w'	– temperature at the plate
T_∞'	– temperature of the fluid far away from the plate
t'	– dimensional time s
u	– dimensionless velocity
u'	– velocity of the fluid in the x' - direction ms^{-1}
β	– volumetric coefficient of thermal expansion K^{-1}
β^*	– volumetric coefficient of concentration expansion K^{-1}
δ	– chemical reaction parameter
θ	– dimensionless temperature
λ	– radiation parameter
ν	– kinematic viscosity m^2s^{-1}
ρ	– fluid density kgm^{-3}
σ	– electrical conductivity
τ	– dimensionless skin-friction $kg m^{-1}s^{-1}$
ϕ	– dimensionless concentration

Subscripts

w	– condition at the wall
∞	– free stream condition

References

- [1] Das U.N., Dekha R. and Soundalgekar V.M. (1994): *Effects of mass transfer on flow past an impulsively started infinite vertical plate with constant heat flux and chemical reaction*. – Forschung im Ingenieurwesen, vol.60, No.10, pp.284-287.
- [2] Muthucumaraswamy R. and Ganesan P. (2001): *Effects of chemical reaction and injection on flow characteristics in an unsteady upward motion of an isothermal plate*. – J. of Appl. Mech. and Theoret. Physics, vol.42, No.4, pp.665-671.

- [3] Chamkha A.J. (2003): *MHD flow of a uniformly stretched vertical permeable surface in the presence of heat generation/absorption and a chemical reaction*. – Int. Comm. in Heat and Mass Transfer, vol.30, No.3, pp.413-422.
- [4] Kandasamy R., Periasamy K. and Prabhu K.K.S. (2005): *Effects of chemical reaction, heat and mass transfer along a wedge with heat source and concentration in the presence of suction or injection*. – Int. J. of Heat and Mass Transfer, vol.48, No.7, pp.1388-1394.
- [5] Muthucumaraswamy R. and Meenakshisundaram S. (2006): *Theoretical study of chemical reaction effects on vertical oscillating plate with variable temperature*. – Theoret. J. of Appl. Mech., vol.33, pp.245-257.
- [6] EL-Kabier S.M.M. and Abdou M.M.M. (2007): *Chemical reaction, heat and mass transfer on MHD flow over a vertical isothermal cone surface in micro-polar fluids with heat generation/absorption*. – Applied Mathematical Sciences, vol.1, No.34, pp.1663-1674.
- [7] AL-Odat M.Q. and AL-Azab T.A. (2007): *Influence of chemical reaction on transient MHD free convection over a moving vertical plate*. – Emirates J. for Engg. Res., vol.12, No.3, pp.15-21.
- [8] Mahapatra N., Dash G.C., Panda S. and Acharya M. (2010): *Effects of chemical reaction on free convection flow through a porous medium bounded by a vertical surface*. – J. of Engg. Phy. and Thermo-Physics, vol.83, No.1, pp.130-140.
- [9] Chamkha A.J. and Ahmed S.E. (2011): *Similarity solution for unsteady MHD flow near a stagnation point of a three dimensional porous body with heat and mass transfer, heat generation/absorption and chemical reaction*. – J. Appl. Fluid Mech., vol.4, No.2, pp.87-94.
- [10] Devika B., Satyanarayana P.V. and Venkataramana S. (2013): *MHD oscillatory flow of a visco-elastic fluid in a porous channel with chemical reaction*. – Int. J. of Engg. Sci. Invention, vol.2, No.2, pp.26-35.
- [11] Grief R., Habib I.S. and Lin J.C. (1971): *Laminar convection of a radiating gas in a vertical channel*. – J. of Fluid Dynamics, vol.46, pp.513-520.
- [12] Ali M.M., Chen T.S. and Armaly B.F. (1984): *Natural convection radiation interaction in boundary layer flow over horizontal surface*. – AIAA Journal, vol.22, No.2, pp.797-803.
- [13] Mansor M.A. (1990): *Radiative and free convection effects on the oscillatory flow past a vertical plate*. – Astrophysics and Space Science, vol.166, pp.269-275.
- [14] ABD-El-Naby M.A., Elbarbary M.E. and Abdelzem N.Y. (2003): *Finite difference solution of radiation effects on MHD free convection flow over a vertical plate with variable surface temperature*. – J. of Applied Mathematics, vol.2, pp.65-86.
- [15] Chandrakala P. and Antony Raj S. (2008): *Radiation effects on MHD flow past an impulsively started infinite isothermal vertical plate*. – Indian J. of Chem. Technology, vol.15, pp.63-67.
- [16] Ahmed N. and Sarmah H.K. (2009): *Thermal radiation effects on a transient MHD flow with mass transfer past an impulsively fixed infinite vertical plate, International* – J. of Appl. Math. and Mech., vol.5, No.5, pp.87-98.
- [17] Mukhopadhyay S. (2009): *Effects of thermal radiation on unsteady mixed convection flow and heat transfer over a porous stretching surface in porous medium*. – Int. J. of Heat and Mass Transfer, vol.52, pp.413-422.
- [18] Anand Rao J. and Prabhakar Reddy B. (2010): *Finite element analysis of heat and mass transfer of an unsteady MHD natural convection flow of a rotating fluid past a vertical porous plate in the presence of radiative heat transfer*. – J. of Energy, Heat and Mass Transfer, vol.32, pp. 223-241.
- [19] Seth G.S., Ansari M.S. and Nandkeolyar R. (2011): *MHD natural convection flow with radiative heat transfer past an impulsively moving plate with ramped wall temperature*. – Heat and Mass Transfer, vol.47, No.5, pp.551-561.
- [20] Muthucumaraswamy R. and Sivakumar P. (2016): *MHD flow past a parabolic flow past an infinite isothermal vertical plate in the presence of thermal radiation and chemical reaction*. – Int. J. of Appl. Mech, and Engg., vol.21, No.1, pp.95-105.

Received: May 24, 2018

Revised: July 13, 2019